Sequential extraction, structural characterization, and antioxidant activity of polysaccharides from *Dendrocalamus brandisii* bamboo shoot shell

Xiaowei Peng [a], Jingjie Liu [a], Ni Tang [a], Jia Deng [b], Can Liu [a], Huan Kan [b], Ping Zhao [a,b], Xia Zhang [c], Zhengjun Shi [a,*], Yun Liu [a,b,*]

[a] *Key Laboratory of State Forestry and Grassland Administration on Highly-Efficient Utilization of Forestry Biomass Resources in Southwest China, Southwest Forestry University, Kunming 650224, China*
[b] *Key Laboratory of Forest Resources Conservation and Utilization in the Southwest Mountains of China Ministry of Education, Southwest Forestry University, Kunming 650224, China*
[c] *School of Pharmacy, Guizhou University, Guiyang 550025, China*

ARTICLE INFO

ABSTRACT

Polysaccharides including water-soluble fraction (W), 1,2-Cyclohexanediaminetetraacetic acid (CDTA)-soluble fraction (CA), sodium carbonate (Na_2CO_3)-soluble fraction (SC), 1 M potassium hydroxide (KOH)-soluble fractions (PH1), and 4 M KOH-soluble fraction (PH4) were successively extracted from *Dendrocalamus brandisii* bamboo shoot shells using water, CDTA, Na_2CO_3, and KOH solution. The analytical methods were employed to initially identify the structural characteristics of the five polysaccharide fractions, and their antioxidant capacities *in vitro* were determined. According to the data, the average molecular weight of the five polysaccharide fractions was between 4 816 and 993 935 Da. In all four types (CA, SC, PH1, and PH4), xylose was the most abundant monosaccharide, especially in PH1 and PH4. Both PH1 and PH4 were found to contain 1,4-β-D-Xyl*p* as their main chain, as determined by nuclear magnetic resonance (NMR) spectroscopy. Additional research into CA and SC's antioxidant potential is required since they both showed potent *in vitro* antioxidant activities.

1. Introduction

The bamboo shoots of *Dendrocalamus brandisii*, which belongs to the genus *Dendrocalamus* of the family Gramineae, are high in protein, carbohydrates, crude fiber, amino acids, minerals, and other nutrients. The name "sweet bamboo shoots" is derived from the fact that *D. brandisii* bamboo shoots are slightly sweet and immediately edible. The majority of them are produced in the Yunnan province of China, specifically in the cities of Simao and Xishuangbanna; however, they are also produced in other countries such as India, Myanmar, Nepal, Sikkim, Bhutan, and Laos (He, Zheng, Chen, Rong, & Zheng, 2020). The majority of fresh *D. brandisii* bamboo shoots in China are used in the food industry as raw materials or semi-finished products. During the process of harvesting bamboo shoots, a significant amount of bamboo shoot shells are either thrown away or burned as waste, which contributed to the worsening of environmental conditions and results in a loss of useful resources (Liu et al., 2018). According to several studies, the shells of *D. brandisii* bamboo shoots contained an abundance of substances that

are beneficial to one's nutrition and health, including dietary fiber, polysaccharides, flavonoids, and phytosterols (He, et al., 2016). Furthermore, it has been confirmed in the literature that the β-pyran polysaccharide and arabinogalactan in bamboo shoot shells may have a hypoglycemic effect (Liu et al., 2018), and the dietary fibers possessed the great water-holding capacity and high binding capacities for oils, nitrite ions, glucose, and cholesterol (Luo et al., 2018). However, no studies on the structural analysis and antioxidant activity of *D. brandisii* bamboo shoot shell polysaccharides have been reported. Because of this, the shells of *D. brandisii* bamboo shoots have a lot of potential for development and use in the field of bioactivity.

In recent years, the exploration of polysaccharides from plant cell walls has gained increasing attention. Polysaccharides in plant cell walls exist not in free form, but are tightly bound to cellulose (hemicellulose) through hydrogen or covalent bonds, resulting in the incomplete separation by traditional and single extraction methods, hence sequential extraction is a more suitable extraction method for plant cell wall polysaccharide (Li, Li, Li, Xu, Yuan, & Cao, 2019). It is common practice

to employ water, 1,2-cyclohexanediaminetetraacetic acid (CDTA), sodium carbonate (Na$_2$CO$_3$), and potassium hydroxide (KOH) as the chemical reagents for successive extraction. Neutral carbohydrates in bamboo shoot shells can be dissolved in water (Houben, Jolie, Fraeye, Loey, & Hendrickx, 2011). The pectic polysaccharides would be freed once CDTA broke the calcium bridges in the cell wall that were cross-linked with them (Li, Li, Li, Xu, Yuan, & Cao, 2019). Then, the pectic polysaccharides that are covalently bonded to cellulose or hemicellulose might be extracted using Na$_2$CO$_3$. To conclude, KOH can be used to remove the hemicellulose from the bamboo shoot shells. Accordingly, the extraction solution for the sequential extraction of polysaccharides from *D. brandisii* bamboo shoot shells was comprised of water, 0.1 M CDTA, 0.05 M Na$_2$CO$_3$, 1 M KOH, and 4 M KOH in this investigation.

Polysaccharides are polymers composed of monosaccharide residues linked by glycosidic bonds (Ren, Bai, Zhang, Cai, & Flores, 2019). Numerous studies have demonstrated that plant polysaccharides possessed biological properties such as antioxidant, hypoglycemic, hypolipidemic, antitumor, anti-fatigue, anti-aging, anti-bacterial, and anti-radiation (Peng et al., 2022; Wu, Zheng, Xia, & Kan, 2015). As was well known, the biological functions of active ingredients were closely related to their structural characteristics. Consequently, it is essential to analyze the structure of polysaccharides before investigating their biological activity.

To our knowledge, there is almost no research on the sequential extraction process, structural characterization and antioxidant capacity of polysaccharides from *D. brandisii* bamboo shoot shells. To elucidate the effects of different extraction solvents on the structure and antioxidant capacity of polysaccharides, five fractional polysaccharides were first extracted from the bamboo shoot shells, a byproduct of processing *D. brandisii* bamboo shoots: the water-soluble fraction (W), the CDTA-soluble fraction (CA), the Na$_2$CO$_3$-soluble fraction (SC), the 1 M KOH-soluble fraction (PH1), and the 4 M KOH-soluble fraction (PH4). The structures of five polysaccharides were characterized and then that information was used to evaluate their *in vitro* antioxidant capabilities.

2. Materials and methods

2.1. Materials and reagents

The bamboo shoot shells belonging to *D. brandisii* were collected in Xishuangbanna, Yunnan Province, China.

All the monosaccharide standards were acquired from Shanghai Yuanye Bio-Technology Co., Ltd. (Shanghai, China). CDTA, Na$_2$CO$_3$, KOH, ascorbic acid (Vc), 1, 1-diphenyl-2-picrylhydrazyl (DPPH), and 2,2′-azino-bis-(3-ethylbenzthiazoline-6-sulphonic acid) (ABTS) were purchased from Tianjin Kemiou Chemical Reagent Co., Ltd. (Tianjin, China). All other chemicals and reagents were purchased from Guangdong Guanghua Sci-Tech Co., Ltd. (Guangdong, China).

2.2. Pretreatment of bamboo shoot shells

The bamboo shoot shells were washed, sorted, heat-pump-dried at 50 °C, crushed, and sieved in a 40-mesh screen. The pigment and phenolic were washed away twice by soaking 200 g of the powder in 2.0 L of 95% (v/v) ethanol at 25 °C for 4 h. The oligosaccharides were then washed away by repeatedly washing the residues with 1.5 L of 70% (v/v) ethanol. The residues that were insoluble in ethanol were then collected, dried, and taken to use in the next procedure.

2.3. Sequential extraction of bamboo shoot shells polysaccharides

The steps involved in the sequential extraction of bamboo shoot shell polysaccharides are depicted in Fig. 1. The W was prepared by repeating the extraction of the ethanol-insoluble residue with a 1:30 w/v ratio of deionized water, centrifuging the supernatant, precipitating with four volumes of 95% (v/v) ethanol, and finally lyophilizing the mixture. Next, the water-insoluble residues were extracted with a 0.1 M CDTA solution (pH 6.6) at a ratio of 1:20 (w/v) for 6 h at 25 °C to yield the CA. After that, the CDTA-insoluble residues were extracted with a 0.05 M Na$_2$CO$_3$ solution containing 0.025 M NaBH$_4$ at a ratio of 1:30 (w/v) to obtain SC. Then, a 1 M KOH solution containing 0.025 M NaBH$_4$ and a 4 M KOH solution containing 0.025 M NaBH$_4$ was used to extract the residues at a ratio of 1:30 (w/v), yielding PH1 and PH4, respectively. For a total of 6 h at 25 °C, each extraction step was repeated twice.

2.4. Total carbohydrate and protein content analysis

The phenol–sulfuric acid technique was used to measure the total carbohydrate content of five polysaccharide fractions (W, CA, SC, PH1, and PH4) (Dubois, Gilles, Hamilton, Rebers, & Smith, 1956). The standard curve equation was $y = 11.327x – 0.0446$ with an R^2 value of 0.9982, where the glucose was used as the standard. The Coomassie Brilliant blue staining was used to assess the protein content of five polysaccharide fractions (Li, Zhao, & Jiang, 2020). Bovine serum albumin was used as a reference, and the equation for the standard curve was $y = 6.08x + 0.0082$, with an R^2 value of 0.9991.
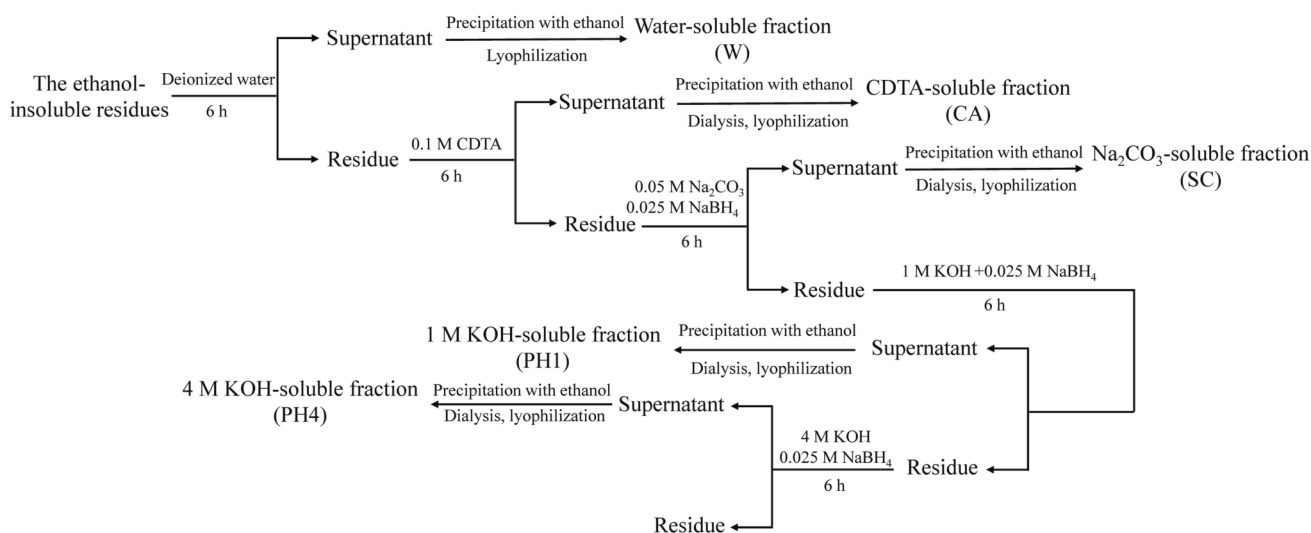

Fig. 1. Extraction process chart for W, CA, SC, PH1, and PH4.

2.5. Molecular weight and monosaccharide composition analysis

The molecular weights of the polysaccharide fractions (W, CA, SC, PH1, and PH4) were determined using high-performance gel permeation chromatography (HPGPC, LC-10A, Shimadzu, Japan) with a refractive index detector and a Gel chromatography column (BRT105-104–102, BoRui Saccharide, China). Ion chromatography (IC, ICS5000, Thermo Fisher, USA) was used to determine the monosaccharide concentrations in five different polysaccharide fractions following a previously reported method with some minor adjustments (Yu, Ji, & Liu, 2018). Trifluoro-acetic acid (TFA) (2 M) in a volume of 10 mL was used to dissolve 5 mg of polysaccharides, and then the mixture was heated to 120 °C for 3 h before being dried in a nitrogen gas stream. The hydrolyzed sample was then mixed with 5 mL of deionized water using a vortex, and 100 μL of the resultant solution was further diluted using deionized water (900 μL). After centrifuged, the supernatant was examined using an IC fitted with an electrochemical detector and a DionexCarbopacTMPA20 column (3 × 150 mm). The mobile phases consisted of H_2O, 250 mM sodium hydroxide (NaOH), 50 mM NaOH, and 500 mM sodium acetate (NaOAc), all flowing at a rate of 0.3 mL·min^{-1}. The sampling volume was 5 μL, and the column temperature was 30 °C.

2.6. Fourier transform infrared (FT-IR) and ultraviolet–visible (UV–vis) spectroscopy analysis

Using a Fourier transform infrared (FT-IR) spectrometer, the chemical bonds, and functional groups of five polysaccharide fractions (W, CA, SC, PH1, and PH4) were determined (IS50, Thermo Scientific, USA). A flake was created by pressing 2 mg of polysaccharides with 200 mg of KBr. The flake was then scanned between 4000 and 500 cm^{-1} in wavelength (Yang, Gao, & Yang, 2020). A spectrophotometer was used to perform a scan at a wavelength range of 200–400 nm across the UV–vis spectra of 1 mg·mL^{-1} polysaccharide aqueous solutions (UV-2600, Shimadzu, Japan).

2.7. X-ray diffraction spectroscopy analysis

In order to acquire X-ray diffraction spectra of polysaccharides, an X-ray diffractometer (UItima IV, Rigaku, Japan) equipped with Cu Kα radiation was used. The scanning rate was set at 5°·min^{-1}, and the 2θ range of 10–70 °.

2.8. Congo red analysis

Using the Congo red method, the conformation of five polysaccharide fractions (W, CA, SC, PH1, and PH4) was established (Xu, Wang, Xue, Pan, & Chen, 2021). Briefly, 3.0 mL of Congo red solution (80 μmol·L^{-1}) was combined with 3.0 mL of polysaccharide solution (1 mg·mL^{-1}). Each of the following concentrations was prepared by adding NaOH solution (1 mol·L^{-1}) to the initial solution: 0, 0.1, 0.2, 0.3, 0.4, and 0.5 mol·L^{-1}. A UV–vis spectrophotometer was then used to determine the maximum absorption wavelength of the solution between 300 and 700 nm.

2.9. Nuclear magnetic resonance (NMR) spectroscopy analysis

NMR spectroscopy was used to understand more about the structures of W, CA, SC, PH1, and PH4. A Bruker 500 MHz NMR spectrometer (AVANCE NEO 500, Bruker, Switzerland) was used to acquire 1D and 2D NMR spectra, specifically ^1H, ^{13}C, Heteronuclear single quantum coherence (HSQC), and H—H COSY (Correlation spectroscopy), by dissolving 20 mg of polysaccharides in 0.55 mL of D_2O (99.9%).

2.10. Scanning electron microscopy (SEM) analysis

The microstructure of the five polysaccharides was studied using

SEM (Regulus8100, Hitachi, Japan). External surfaces of the samples (2 mg) were scanned using electron microscopy at a voltage of 5.0 kV after being sputtered with a gold coating and placed on aluminum holders.

2.11. Antioxidant activity assays

2.11.1. DPPH radical scavenging activity

Slight adjustments were made to the reported procedure to assess the scavenging effect on the DPPH radical (Peng et al., 2022). 2 mL of the sample solution (0.2–1.0 mg·mL^{-1}) was mixed with 2 mL of the DPPH radical ethanol solution (0.1 mmol·L^{-1}). After letting the combinations remain in dark at 37 °C for 30 min, the absorbance was measured at 517 nm with Vc serving as a positive control. The formula for the computation proceeded as follows:

$$Effect\ (\%)\ =\ [1 - (A_1 - A_2)/A_0] \times 100\%$$

where A_1 indicates the sample absorbance mixed with DPPH ethanol solution, A_0 denotes the distilled water absorbance replacing the sample, and A_2 represents the ethanol absorbance replacing DPPH.

2.11.2. ABTS radical scavenging activity

The effect of scavenging on ABTS radicals was evaluated using a modified version of the approach reported by Zhu et al. (2022). After mixing the ABTS radical solution (7.0 mmol·L^{-1}) with the $K_2S_2O_8$ solution (5 mmol·L^{-1}) and letting it sit for 12 h at room temperature in the dark to obtain the ABTS radical cation solution. Then, ethanol was added until the absorbance at 734 nm was 0.70 ± 0.02. A total of 3 mL of ABTS radical cation solution was added to 1 mL of the diluted sample solution (0.1–0.5 mg·mL^{-1}). After waiting 5 min at room temperature in the dark, the absorbance at 734 nm was measured using Vc as a reference. The formula for the computation proceeded as follows:

$$Effect\ (\%)\ =\ [1 - (A_1 - A_2)/A_0] \times 100\%$$

where A_1 indicates the sample absorbance mixed with ABTS solution, A_0 denotes the distilled water absorbance replacing the sample, and A_2 represents the distilled water absorbance replacing ABTS solution.

2.11.3. OH radical scavenging activity

Minor adjustments were made to the outlined approach in order to assess the •OH radical scavenging effect (Deng et al., 2021). 2 mL of a sample solution (1.0–5.0 mg·mL^{-1}) was combined with 2 mL of a hydrogen peroxide solution (30% v/v), 2 mL of a salicylic acid–ethanol solution (9 mmol·L^{-1}), and 2 mL of $FeSO_4$ (9 mmol·L^{-1}) at 37 °C for 30 min. Then the absorbance was measured at 510 nm using Vc as a positive control. The formula for the computation proceeded as follows:

$$Effect\ (\%)\ =\ [1 - (A_1 - A_2)/A_0] \times 100\%$$

where A_1 indicates the sample absorbance, A_0 and A_2 denote the distilled water absorbance instead of sample or hydrogen peroxide, respectively.

2.12. Statistical analysis

Origin 2018 was used to process the images. All data were expressed as mean ± standard deviation (SD). Student's *t*-test was used at a significance level of $p < 0.05$ for multiple comparison tests.

3. Results and discussion

3.1. Yield, total carbohydrate, and protein content

Five polysaccharide fractions of W, CA, SC, PH1, and PH4 obtained from *D. brandisii* bamboo shoot shells were listed in Table 1. The percent yield of W, CA, SC, PH1, and PH4 was found to be 1.27%, 1.15%, 0.83%,

Table 1
The yield, total carbohydrate content, protein content, Mw, and monosaccharide compositions of five polysaccharide fractions.

Samples	W	CA	SC	PH1	PH4
Yield (%)	1.27	1.15	0.83	10.82	5.23
Total carbohydrate (%)	62.52 ± 1.10	74.07 ± 0.69	78.55 ± 2.58	92.02 ± 0.01	96.96 ± 0.01
Protein (%)	6.35 ± 0.09	9.15 ± 0.06	9.35 ± 0.22	4.16 ± 0.22	3.52 ± 0.76
Mw (Da)	1.06×10^5	i)4.42×10^4 ii)1.04×10^4 iii)4.82×10^3	i)1.60×10^4 ii)8.83×10^3 iii)5.25×10^3	1.40×10^5	i)9.94×10^5 ii)2.53×10^4
Mn (Da)	6.73×10^4	i)3.00×10^4 ii)7.84×10^3 iii)3.85×10^3	i)1.17×10^4 ii)6.75×10^3 iii)4.16×10^3	8.72×10^4	i)5.38×10^5 ii)1.79×10^4
Mw/Mn	1.58	i)1.47 ii)1.33 iii)1.25	i)1.37 ii)1.31 iii)1.26	1.61	i)1.85 ii)1.41
Monosaccharide composition (mol%)					
Galactosamine	–	1.4	–	–	–
Rhamnose	–	3.0	–	–	–
Arabinose	32.4	24.5	25.6	11.9	10.3
Glucosamine	1.2	2.2	0.7	–	–
Galactose	43.3	12.2	8.6	1.9	1.8
Glucose	7.4	4.5	3.7	3.4	5.6
Xylose	1.6	47.3	57.8	82.9	82.3
Galacturonic acid	4.1	5.8	3.6	–	–

10.82%, and 5.23%, respectively. The results indicated that bamboo shoot shells were rich in loosely bonding and tightly bonding hemicellulose, particularly loosely bonding hemicellulose. Furthermore,

bamboo shoot shells have also been proven to be an excellent source of dietary fiber due to the richness of hemicellulose and cellulose (Li, Li, Li, Xu, Yuan, & Cao, 2019). Hemicellulose polysaccharides were mainly enriched in bamboo shoot shells to maintain the stability of the cell wall structure, as reported by Houben et al. (2011).

As presented in Table 1, the total carbohydrate content of W, CA, SC, PH1, and PH4 was $62.52 \pm 1.10\%$, $74.07 \pm 0.69\%$, $78.55 \pm 2.58\%$, $92.02 \pm 0.01\%$, and $96.96 \pm 0.01\%$, corresponding to the protein content was $6.35 \pm 0.09\%$, $9.15 \pm 0.06\%$, $9.35 \pm 0.22\%$, $4.16 \pm 0.22\%$, and $3.52 \pm 0.76\%$, respectively. A portion of non-carbohydrates such as proteins in bamboo shoot shells was previously dissolved into water, CDTA, and Na_2CO_3 solutions, resulting in higher purity of sugars in PH1 and PH4 than in W, CA, and SC.

3.2. Molecular weights and compositions of monosaccharides

The molecular weight of five polysaccharides was listed in Table 1 and Fig. 2A. W and PH1 both exhibit a single signal of molecular weight (Mw), indicating that they were chemically homogenous, with weight average Mw of 1.06×10^5 and 1.40×10^5 Da, respectively. However, CA, SC, and PH4 were found to contain two or three signals, demonstrating that they all have multiple polysaccharide fragments of different molecular weights. Specifically, the Mw of CA was 4.42×10^4, 1.04×10^4, and 4.82×10^3 Da; the Mw of SC was 1.60×10^4, 8.83×10^3, and 5.25×10^3 Da; the Mw of PH4 was 9.94×10^5 and 2.53×10^4 Da, respectively. As shown above, the Mw of W, CA and SC were lower than PH1 and PH4. The reason can be attributed to the strong alkali destroying more covalent bonds in the cell wall and increasing the solubility of large Mw polysaccharides. According to some reported studies, polysaccharides with a low Mw may exhibit greater *in vitro* antioxidant activity (Sheng & Sun, 2014). Furthermore, CA and SC also have lower dispersion based on the dispersion index (Mw/Mn) in Table 1 compared to W, PH1, and PH4, indicating that they have less

Fig. 2. Characterization of five polysaccharide fractions. HPGPC chromatogram (A). The peaks with a retention time of about 46 min were created by the mobile phase. Ion chromatogram (B). 1. fucose; 2. galactosamine; 3. rhamnose; 4. arabinose; 5. glucosamine; 6. galactose; 7. glucose; 8. N-Acetyl-D-Glucosamine; 9. xylose; 10. mannose; 11. fructose; 12. ribose; 13. galacturonic acid; 14. guluronic acid; 15. glucuronic acid; 16. mannuronic acid. FT-IR spectrum (C). UV–vis spectrum (D). Maximum absorption wavelength of the Congo red–polysaccharide complex at various concentrations of NaOH (E). (For interpretation of the references to colour in this figure legend, the reader is referred to the web version of this article.)

branches.

As shown in Table 1 and Fig. 2B, there were obvious differences in the compositions of the monosaccharides containing in the five polysaccharide fractions. Arabinose, galactose, glucose, and xylose were detected in all five polysaccharides. While galacturonic acid and glucosamine were only found in W, CA, and SC. Moreover, galactosamine and rhamnose were only revealed in CA. Furthermore, arabinose (32.4%) and galactose (43.3%) were the principal monosaccharides in W, similar to the results reported by Yu et al. (2022). Xylose was the major monosaccharide in CA, SC, PH1, and PH4 with 47.3%, 57.8%, 82.9%, and 82.3%, respectively. Meanwhile, the molar ratio of arabinose in CA and SC was also relatively high, reaching 24.5% and 25.6%, respectively. Xylose is a crucial part of the hemicellulose and does not exist in its free form. Agricultural waste products are considered one of the major sources of xylose (Zhang, Yu, & Yu, 2020). From the aforementioned, it was found that except for W, all four polysaccharides contained significant amounts of xylose.

3.3. FT-IR and UV–vis spectroscopy

The critical chemical bonds and functional groups of bamboo shoot shell polysaccharides could be tentatively determined using FT-IR spectroscopy. As depicted in Fig. 2C, the infrared spectra of the five polysaccharide fractions exhibited minor differences in intensity and individual absorption peaks between 4000 and 500 cm^{-1}. Characteristic peaks of polysaccharides include a broad, intense peak at 3369 cm^{-1} and a peak at 2935 cm^{-1}, which have been related to the O—H and C—H stretching vibration, respectively (Chen, Chen, Zhang, Chen, Hu, & Kan, 2018; Yang, Yang, & Yang, 2018). The CA spectrum's absorption at 1727 cm^{-1}, which is associated with the methylated carboxyl (COO-R) group, can be utilized to assess the level of esterification of polysaccharides (Chatjigakis, Pappas, Proxenia, Kalantzib, Rodis, & Polissiou, 1998). However, similar peaks were not detected in the other samples. The two absorption bands at 1640 cm^{-1} and 1416 cm^{-1} were regarded as the C=O stretching vibration and C—H bending vibration of uronic acid, accordingly. In Fig. 2C, the obvious absorption peak at 1416 cm^{-1} was found only in W, CA, and SC, implying the absence of uronic acid in PH1 and PH4, which was consistent with the detection results of the monosaccharide compositions. Furthermore, the absorption peaks between 1167 and 1068 cm^{-1} of PH1 and PH4 represented the bending of xylan C—C or C—O or C—O—H vibrations (Liu et al., 2022). Therefore, xylan was the major component of PH1 and PH4 through a comprehensive analysis. The stretching vibration at 1041 cm^{-1} was derived from the C—O—C bond. Consequently, the typical
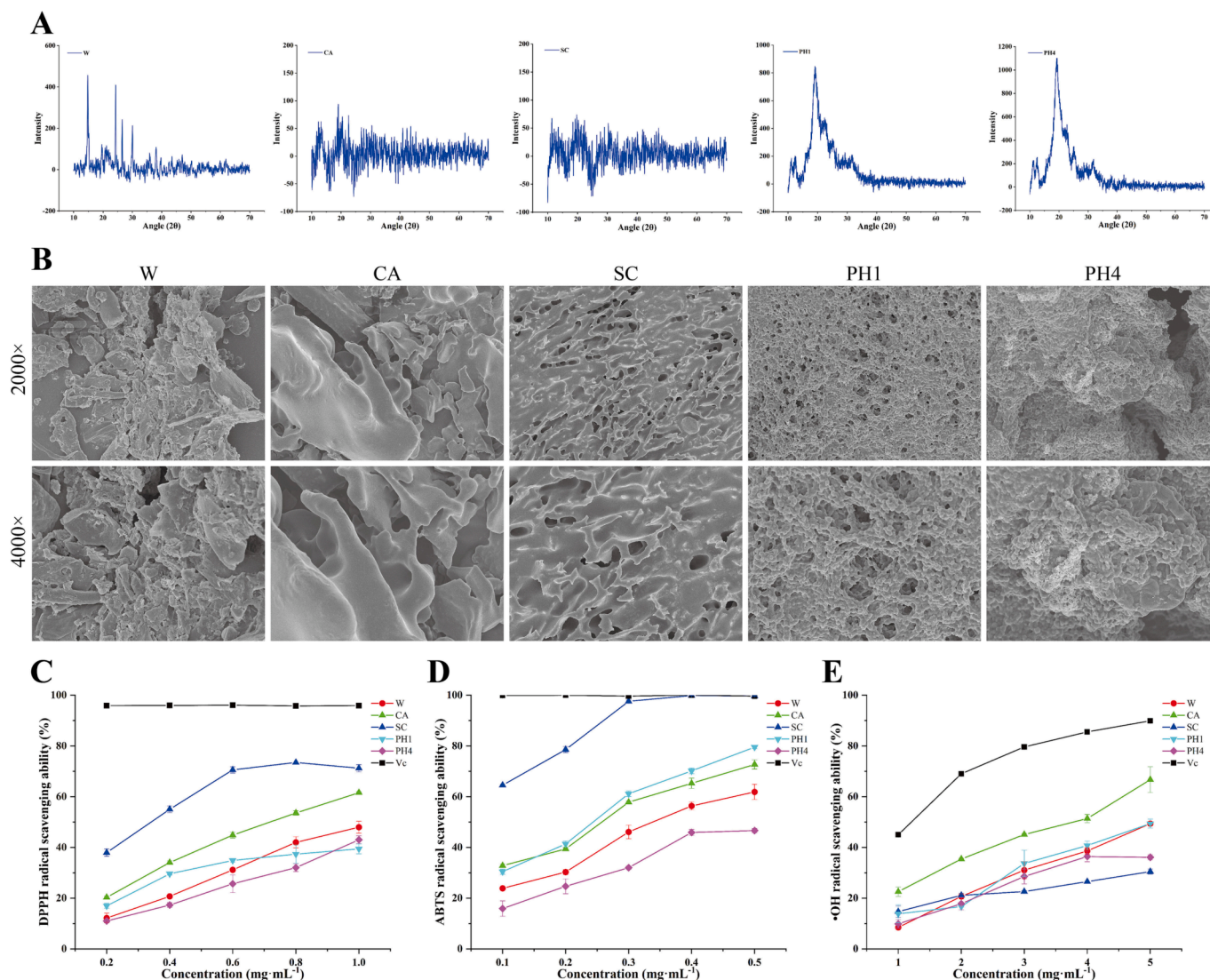
Fig. 3. X-ray diffraction spectrum of five polysaccharide fractions (A). SEM images of W, CA, SC, PH1, and PH4 (B). DPPH radical scavenging rate (C). ABTS radical scavenging rate (D). •OH radical scavenging rate (E).

absorption peaks at 898 cm^{-1} and 981 cm^{-1} indicated α-type and β-type glycosidic linkages, respectively (Guo et al., 2022).

The residual proteins and nucleic acids in samples could be detected by UV–vis spectroscopy at 280 nm and 260 nm, respectively. As shown in Fig. 2D, all five polysaccharide fractions showed a distinct peak at near 280 nm, indicating that they contained a certain amount of protein. Among them, the highest absorption of SC indicated the highest protein content, which was almost consistent with the results of the Coomassie Brilliant blue method. Additionally, there was no 260 nm absorption signature, proving that none of the five samples contained any nucleic acids.

3.4. X-ray diffraction spectroscopy

Crystal structural elucidation of plant polysaccharides can be done with high precision using X-ray diffraction, and the degree to which a polysaccharide is crystalline can be used to make predictions about its solubility, swelling capacity, and melting point (Lee et al., 2019). As shown in Fig. 3A, W exhibited diffraction peaks at 14.86°, 24.28°, 26.50°, and 30.02°, indicating that it was a semi-crystalline polymer. Similar findings have been reported before (Chen, Li, Wang, Mei, Zhang, & Kan, 2019). CA and SC had no significant peaks in the range of 10° to 70°, suggesting a non-crystalline structure. PH1 and PH4 show a sharp and strong peak at 19.20° and 19.28°, respectively, indicating that there were both amorphous and crystalline parts in their structures (Mutaillifu et al., 2020; Nuerxiati et al., 2019).

3.5. Congo red

The functional properties and biological activities of polysaccharides were influenced by their triple helix conformation (Feng et al., 2022). The Congo red test is frequently used to infer the triple helix conformation of polysaccharides, as it forms a complex with polysaccharides with a triple helix conformation, increasing the maximum absorption wavelength in solution. A high concentration of NaOH solution would destroy the hydrogen bonds of the triple helix structure, resulting in a reduction of the maximum absorption wavelength of the complex (Guo et al., 2018). As shown in Fig. 2E, none of the maximum absorption wavelengths of the five polysaccharide-Congo red solutions decreased with increasing NaOH concentration compared with control experiment. This data suggested that the five polysaccharides may not have a triple helix shape. It has been shown that strong alkalis, chelating agents, and carbonates had a disruptive effect on hydrogen bonds, thus reducing the stability of the triple helix structure (Feng et al., 2022).

3.6. NMR

NMR spectroscopy can be used to explore the primary structure of polysaccharides with a very low sample amount (Li, Tian, Jiang, Lin, Liu, & Yang, 2021). The anomeric protons of α-configuration mostly appear between δ 4.9–5.5 ppm and 95–103 ppm, and the anomeric protons of β-configuration correspond relatively to the region of δ 4.3–4.9 ppm and 103–110 ppm.

The ^{1}H and ^{13}C NMR spectra of W were shown in Fig. 4A and 4B, with anomeric proton signals at δ 5.06 ppm and anomeric carbon signals at δ 109.15, 107.31, and 103.05 ppm. According to HSQC (Fig. 4C) and ^{1}H–^{1}H COSY (Fig. 4D) spectra, signals at δ 5.06/109.15 (H1/C1), 4.04/81.23 (H2/C2), 3.96/80.80 (H3/C3), 4.10/82.30 (H4/C4), 3.96/68.38 (H5/C5), and 3.76/68.59 ppm (H6/C6) were assigned to 1,5-α-L-Ara$f$, and signals at δ 4.38/103.05 (H1/C1), 3.49/72.50 (H2/C2), 3.55/75.04 (H3/C3), 3.85/68.38 (H4/C4), 3.76/75.04 (H5/C5), 4.04/68.59 ppm (H6/C6) were contributed to 1,6-β-D-Gal$p$ (Huo et al., 2020). The monosaccharide analysis of W has also showed that arabinose and galactose were the principal monosaccharides.

As shown in Fig. 4, the major anomeric carbon proton signals of CA were δ 5.27, 5.07, 4.94, 4.46, and 4.35 ppm, and the major anomeric carbon signals were δ 101.61, 98.91, 96.58, and 92.18 ppm. In addition, the signals at δ 173.39 ppm (C6) indicated the presence of 1,4-β-D-Gal$p$A, with signals of 4.46/96.58 (H1/C1), 3.12/73.99 (H2/C2), 3.66/76.33 (H3/C3), 3.45/69.18 (H4/C4), 4.29/77.82 (H5/C5), and 173.39 ppm (C6) (Ji, Yan, Hou, Shi, & Liu, 2020). Based on the reported data, the signals in the HSQC spectra of CA were assigned as 1,3-α-Ara$p$ units, 1,6-α-D-Glc$p$ units, 1,4-β-Gal$p$ units, and 1,4-β-D-Xyl$p$ units (Feng et al., 2022; Xia, Liang, Yang, Wang, & Kuang, 2015; Zhu et al., 2022), whose signals were shown in Table 2.

The ^{1}H, ^{13}C, HSQC, and ^{1}H–^{1}H COSY spectra of SC were shown in Fig. 4. The main anomeric carbon proton signals were δ 5.23, 4.42, and 4.33 ppm, and the main anomeric carbon signals were δ 107.60, 101.61, 96.45, and 92.18 ppm. Based on the previously reported data, it was validated that SC contained α-L-Ara$f$ units except for 1,3-α-Ara$p$ units, 1,4-β-Gal$p$ units, and 1,4-β-D-Xyl$p$ units, which were consistent with CA (Zhu et al., 2022). Furthermore, the correlations at δ 5.23/107.06, 3.53/69.83, 3.63/76.73, 3.48/73.03, 3.12/73.24, and 3.31/72.17 ppm were found associated with H1/C1, H2/C2, H3/C3, H4/C4, H5/C5, and H6/C6 signals from α-L-Ara$f$, respectively (Chen, Li, Qing, Chen, Zhang, & Yan, 2020; Zhang, Zhang, Zhang, Wang, & Yan, 2018). The ^{13}C NMR of SC exhibited a significant signal in the range of δ 170–180 ppm, implying the existence of galacturonic acid.

The ^{1}H, ^{13}C, HSQC, and ^{1}H–^{1}H COSY spectra of PH1 and PH4 were shown in Fig. 4. Their main anomeric carbon proton signals were δ 5.23, 4.56, and 4.33 ppm, respectively, and the main anomeric carbon signal was δ 101.61 ppm. According to the spectral data of HSQC and ^{1}H–^{1}H COSY, it was established that both PH1 and PH4 contained 1,4-β-D-Xyl$p$, as shown by the signals 4.33/101.61 (H1/C1), 3.31/73.59 (H2/C2), 3.65/76.27 (H3/C3), 3.58/74.82 (H4/C4), 3.22/62.91 (H5/C5), and 3.51/69.11 ppm (H6/C6) (Liu et al., 2018; Liu et al., 2022; Xiao et al., 2020). Using FT-IR spectroscopy and monosaccharide composition analyses, xylose was found to be present in PH1 and PH4 as the predominant monosaccharide. As a result, 1,4-β-D-Xyl$p$ was initially identified as the primary sugar linking chain in both PH1 and PH4.

3.7. SEM

SEM is considered to be one of the most direct methods for the investigation of polysaccharides morphology. As shown in Fig. 3B, the five polysaccharide fractions showed variations in their apparent morphology. W showed a scattered flake or lump. The morphology of CA was more complete than other polysaccharides, but a few small fragments were present. Moreover, SC's surface was reticulated, with many small holes. Similar to the bamboo leaf polysaccharides examined by Xiao et al. (2020), PH1 and PH4 possessed a homogenous spherical shape with good dispersion, which can also be drawn based on the polysaccharide dispersion index. The cause of this phenomenon may be the strong attraction between macromolecules.

3.8. Antioxidant activity

Since DPPH radical is both stable and sensitive, it is widely used to evaluate the antioxidant capability of active compounds. The ability of Vc and the five polysaccharide fractions to scavenge DPPH radicals at various concentrations were shown in Fig. 3C. All five polysaccharides exhibited significant scavenging activity against DPPH radical dose-dependently. At 1.0 mg·mL^{-1}, the clearance rates of W, CA, SC, PH1, PH4, and Vc were 48.0%, 61.6%, 71.2%, 39.4%, 43.0%, and 95.9%, respectively. These results suggested that SC exhibited stronger DPPH radical scavenging ability than other fractions, which may have some relationship with the uronic acid content. Peng et al. (2022) showed a positive effect of uronic acid on DPPH radical scavenging ability. In addition, Guo et al. (2022) have found that sodium carbonate fraction extracted from sesame hulls also displayed potent DPPH radical scavenging ability.

ABTS radical and potassium persulfate reacted to form a stable blue-
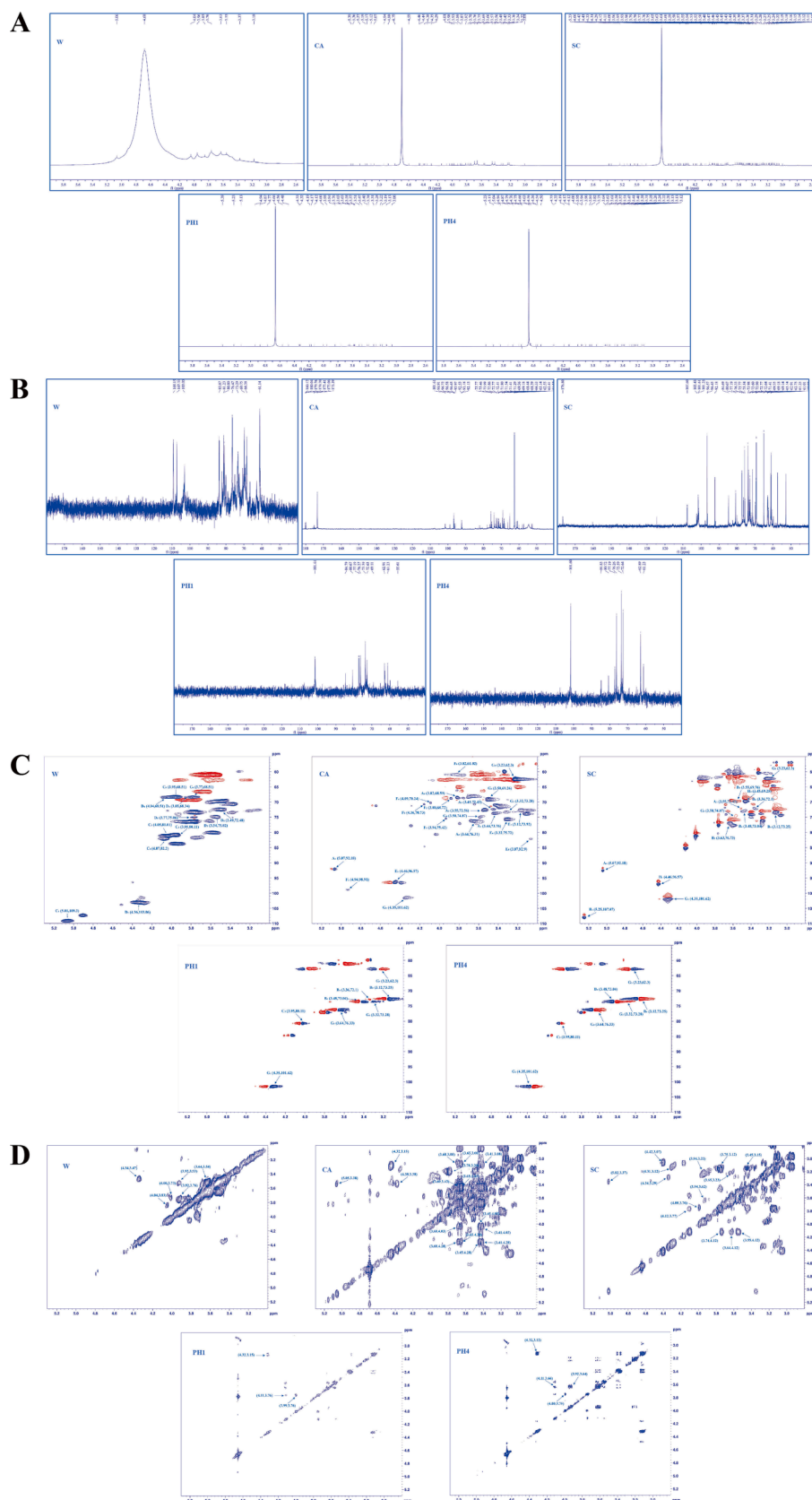
Fig. 4. NMR spectra of five polysaccharide fractions. 1H spectrum (A), 13C spectrum (B), HSQC spectrum (C) and 1H–1H COSY spectrum (D).

Table 2
Chemical shift assignments of ^1H and ^{13}C NMR spectrum of five polysaccharide fractions.

Residue	Sugar linkage	Symbol	δ ^1H/^{13}C (ppm)					
			1	2	3	4	5	6
Ara	←3)-α-Ara*p*-(1→	A	5.07	3.45	3.53	3.45	3.65	3.82
			92.18	72.40	72.64	73.73	76.33	68.56
	α-L-Ara*f*-(1→	B	5.23	3.53	3.63	3.48	3.12	3.31
			107.60	69.83	76.73	73.03	73.24	72.17
	←5)-α-L-Ara*f*-(1→	C	5.06	4.04	3.96	4.10	3.96	3.76
			109.15	81.23	80.80	82.30	68.38	68.59
Gal	←6)-β-D-Gal*p*-(1→	D	4.38	3.49	3.55	3.85	3.76	4.04
			103.05	72.50	75.04	68.38	75.04	68.59
	←4)-β-Gal*p*-(1→	E	4.46	3.12	3.66	3.93	3.08	3.33
			96.58	73.99	76.33	75.46	82.17	75.77
Glc	←6)-α-D-Glc*p*-(1→	F	4.94	3.89	3.93	4.08	4.15	3.82
			98.91	68.70	75.46	70.29	70.77	61.04
Xyl	←4)-β-D-Xyl*p*-(1→	G	4.33	3.31	3.65	3.58	3.22	3.51
			101.61	73.59	76.27	74.82	62.91	69.11
GalA	←4)-β-D-GalA-(1→	H	4.46	3.12	3.66	3.45	4.29	-
			96.58	73.99	76.33	69.18	77.82	173.39

green complex that is discolored by antioxidants. As shown in Fig. 3D, the scavenging ability of the five polysaccharide fractions (0.1–0.5 mg·mL^{-1}) on ABTS radicals was significantly enhanced with increasing concentration. SC demonstrated the most potent scavenging activity among them, and its scavenging ability was close to that of Vc when the concentration reached 0.3 mg·mL^{-1}. Moreover, at 0.5 mg·mL^{-1}, the clearance rates of W, CA, SC, PH1, PH4, and Vc were 61.9%, 72.7%, 99.7%, 79.54%, 46.6%, and 99.6% respectively.

•OH radical is considered harmful for their ability to destroy macromolecules in biological systems, such as nucleic acids, proteins, and lipids (Lin et al., 2018). Five polysaccharide fractions, as shown in Fig. 3E, demonstrated some scavenging activity for •OH radicals, however, they were all less effective than Vc. The clearance rates of W, CA, SC, PH1, PH4, and Vc were 49.4%, 66.7%, 30.5%, 49.4%, 36.1%, and 89.9% at a concentration of 5.0 mg·mL^{-1}, respectively. The scavenging ability of CA for •OH radical was significantly higher than that of the other four fractions, which was consistent with the findings by Guo et al. (2022).

Herein, the five fractions, i.e., W, CA, SC, PH1, and PH4, showed different scavenging abilities for DPPH, ABTS, and •OH radicals. Briefly, the scavenging activity of these fractions on ABTS radical was stronger than that of DPPH and •OH. Among them, SC exhibited significant DPPH and ABTS radical scavenging ability and CA possessed the strongest •OH scavenging ability, which may be connected to the composition of monosaccharides such as galacturonic acid and their low molecular weight (He, Zhang, Zhang, Linhardt, & Sun, 2016). However, the antioxidant capacity of polysaccharides is not the result of individual factors but is influenced by the interaction of several factors (Wang, Mao, & Wei, 2012). Further studies were required to elucidate the correlation between them.

4. Conclusion

In this study, the association between the sequential extraction methods and structural characterization of polysaccharides from *D. brandisii* bamboo shoot shells was elucidated, followed by the investigation of their *in vitro* antioxidant activity. The yield, molecular weight distribution, monosaccharide composition, crystal structure, conformation, and *in vitro* antioxidant activity of bamboo shoot shell polysaccharides were considerably influenced by the extraction process. Particularly, the average molecular weight of the five polysaccharide fractions was between 4 816 and 993 935 Da. The most diverse monosaccharides in CA revealed the highest levels of galacturonic acid and the most potent •OH radical scavenger activity. SC mainly contained β-Xyl and α-L-Ara*f* with the appearance of a reticulated structure. Moreover, SC exhibited potent DPPH and ABTS radical scavenging

activities. Both PH1 and PH4 were composed primarily of β-Xyl, a monosaccharide, and shared a similar spherical structure. Additionally, the structures of W, PH1, and PH4 were found to be semi-crystalline polymers. None of the five polysaccharide fractions had a distinct triple helix structure. Taken together, CA and SC exhibited potent antioxidant scavenging activity. Nevertheless, the association between their structures and *in vitro* antioxidant capacity remained to be further elucidated in some advanced experimental models including the disease animal models. Further, the mechanisms for their antioxidant potentials also need to be explored on the molecular level while employing advanced animal models.

Data availability

Data will be made available on request.

CRediT authorship contribution statement

Xiaowei Peng: Investigation, Data curation, Writing – original draft. **Jingjie Liu:** Data curation. **Ni Tang:** Investigation, Data curation. **Jia Deng:** Methodology, Supervision. **Can Liu:** Methodology, Supervision. **Huan Kan:** Methodology, Investigation. **Ping Zhao:** Methodology, Validation. **Xia Zhang:** Formal analysis. **Zhengjun Shi:** Methodology, Resources, Supervision, Project administration. **Yun Liu:** Conceptualization, Methodology, Resources, Writing – review & editing, Funding acquisition.

Declaration of Competing Interest

The authors declare that they have no known competing financial interests or personal relationships that could have appeared to influence the work reported in this paper.

Data availability

Data will be made available on request.

Acknowledgments